


# Arylsulfatase A deficiency causes seminolipid accumulation and a lysosomal storage disorder in Sertoli cells<sup>§</sup>

Hongbin Xu,<sup>\*,†</sup> Kessiri Kongmanas,<sup>\*,†</sup> Suraj Kadunganattil,<sup>\*,†,§</sup> Charles E. Smith,<sup>\*\*,†</sup> Tony Rupar,<sup>†,§§</sup> Naoko Goto-Inoue,<sup>\*\*\*</sup> Louis Hermo,<sup>\*\*</sup> Kym F. Faull,<sup>††</sup> and Nongnuj Tanphaichitr<sup>1,\*,†,§</sup>

Chronic Diseases Program,<sup>\*</sup> Ottawa Hospital Research Institute, Ottawa, ON K1Y4E9, Canada; Department of Biochemistry/Microbiology/Immunology<sup>†</sup> and Department of Obstetrics/Gynaecology,<sup>§</sup> Faculty of Medicine, University of Ottawa, Ottawa ON K1H8M5, Canada; Department of Anatomy and Cell Biology,<sup>\*\*</sup> McGill University, Montreal, Quebec H3A2B2, Canada; Departments of Pediatrics<sup>††</sup> and Biochemistry,<sup>§§</sup> University of Western Ontario, London, ON N6A5W9, Canada; Department of Molecular Anatomy,<sup>\*\*\*</sup> Hamamatsu University School of Medicine, Shizuoka 431-3192, Japan; and Pasarow Mass Spectrometry Laboratory,<sup>†††</sup> NPI-Semel Institute for Neuroscience and Human Behavior, David Geffen School of Medicine, University of California, Los Angeles, CA 90024

**Abstract** Sulfogalactosylglycerolipid (SGG) is the major sulfoglycolipid of male germ cells. During spermatogenesis, apoptosis occurs in >50% of total germ cells. Sertoli cells phagocytose these apoptotic germ cells and degrade their components using lysosomal enzymes. Here we demonstrated that SGG was a physiological substrate of Sertoli lysosomal arylsulfatase A (ARSA). SGG accumulated in Sertoli cells of *Arsa*<sup>-/-</sup> mice, and at 8 months of age, this buildup led to lysosomal swelling and other cellular abnormalities typical of a lysosomal storage disorder. This disorder likely compromised Sertoli cell functions, manifesting as impaired spermatogenesis and production of sperm with near-zero fertilizing ability in vitro. Fecundity of *Arsa*<sup>-/-</sup> males was thus reduced when they were older than 5 months. Sperm SGG is known for its roles in fertilization. Therefore, the minimal sperm fertilizing ability of 8-month-old *Arsa*<sup>-/-</sup> males may be explained by the 50% reduction of their sperm SGG levels, a result that was also observed in testicular germ cells.  These unexpected decreases in SGG levels might be partly due to depletion of the backbone lipid palmitylpalmitoylglycerol that is generated from the SGG degradation pathway in Sertoli cells and normally recycled to new generations of primary spermatocytes for SGG synthesis.—Xu, H., K. Kongmanas, S. Kadunganattil, C. E. Smith, T. Rupar, N. Goto-Inoue, L. Hermo, K. F. Faull, and N. Tanphaichitr. **Arylsulfatase A deficiency causes seminolipid accumulation and a lysosomal storage disorder in Sertoli cells.** *J. Lipid Res.* 2011. 52: 2187–2197.

**Supplementary key words** spermatogenesis • lysosomes • electron microscopy

Arylsulfatase A (ARSA) is known as a lysosomal enzyme that desulfates saposin B-solubilized sulfoglycolipids, including sulfogalactosylceramide [SGC or sulfatide, 1-*O*- $\beta$ -D-(3'-sulfo)-galactopyranosyl-*N*-acyl-sphingosine], its analog sulfogalactosylglycerolipid [SGG or seminolipid, 1-*O*-alkyl-2-*O*-acyl-3-*O*- $\beta$ -D-(3'-sulfo)-galactopyranosyl-*sn*-glycerol], and small arylsulfates (1). SGC is a physiological substrate of ARSA; it accumulates in the brains of *Arsa*<sup>-/-</sup> mice and of metachromatic leukodystrophy patients with a genetic deficiency of ARSA (2). In the male reproductive system, ARSA is present in the lysosomes of Sertoli cells and in the acrosome of spermatids and sperm (3). In the epididymis, ARSA is secreted by principal cells into the lumen, and subsequently, it binds to the sperm head via its affinity for cell surface SGG (4). However, ARSA binding to SGG on the sperm surface is presumably not at the active site pocket of ARSA, as it does not lead to SGG desulfation (4). We have shown that both surface ARSA and SGG coexist in sperm head lipid rafts (5, 6). Both ARSA and SGG have direct affinity for the zona pellucida (ZP) (5, 7) and thus contribute to the binding of the sperm lipid rafts to the ZP (5).

Abbreviations: ARSA, arylsulfatase A; CGT, ceramide galactosyltransferase; CST, cerebroside sulfotransferase; GALC, galactosylceramidase; MRM, multiple reaction monitoring; PPG, palmitylpalmitoylglycerol; RT, room temperature SGG, sulfogalactosylglycerolipid; SGC, sulfogalactosylceramide; TGC, testicular germ cell; ZP, zona pellucida.

<sup>1</sup>To whom correspondence should be addressed.

e-mail: ntanphaichitr@ohri.ca

<sup>§</sup>The online version of this article (available at <http://www.jlr.org>) contains supplementary data in the form of five figures and two tables.

This work was funded by Canadian Institutes of Health Research (CIHR) MOP 84420 (to N.T.), an Ontario Graduate Scholarship (to H.X.), and the Development and Promotion of Science and Technology (DPST) Talented Project scholarship of Thailand (to K.K.).

Manuscript received 17 August 2011 and in revised form 28 September 2011.

Published, JLR Papers in Press, October 2, 2011

DOI 10.1194/jlr.M019661

Copyright © 2011 by the American Society for Biochemistry and Molecular Biology, Inc.

This article is available online at <http://www.jlr.org>

SGG is a sulfoglycolipid present selectively in mammalian male germ cells at high levels (10 mol% of total cell lipids). The main molecular species, accounting for more than 90% of total SGG in male germ cells, contains C16:0 alkyl and C16:0 acyl chains (8). SGG is synthesized in primary spermatocytes through sequential steps, including galactosylation of alkylacylglycerol (palmitylpalmitoylglycerol, PPG for the main SGG species) by ceramide galactosyltransferase (CGT) to form galactosylglycerolipid (GG), which is then sulfated by cerebroside sulfotransferase (CST) to form SGG (9, 10). The utilization of these two enzymes in the biosynthesis of SGG is the same as that of SGC in the brain (8). Once synthesized, SGG is targeted to the plasma membrane where it remains throughout the developing steps of male germ cells and finally sperm (8). Significantly, SGG is essential for the continuation of spermatogenesis. Mice genetically null for *Cgt* or *Cst* are infertile due to an arrest of spermatogenesis during pachytene spermatocyte development (11, 12).

Although the biosynthetic pathway of SGG has been delineated, the degradation process of SGG in the testis has not been well defined. Degradation of SGG would likely occur on membrane remnants of apoptotic germ cells after phagocytosis by Sertoli cells. It is well known that during spermatogenesis, testicular germ cells (TGC), especially spermatogonia and spermatocytes, undergo apoptosis at a significant rate (>50% of total TGCs) (13) and that Sertoli cells are responsible for phagocytosis and degradation of apoptotic germ cell components (14, 15), including SGG. Like SGC and other glycolipids, elevated intracellular levels of SGG are likely cytotoxic (16). In fact, intracellular buildups of SGC and several other glycolipids are known to cause lysosomal storage disorders (17, 18). Therefore, Sertoli cells would have to degrade SGG into a deglycosylated neutral nontoxic lipid, such as PPG. Based on the known degradation pathway of SGC (8), this would require ARSA to desulfate SGG to form GG, and then galactosylceramidase (GALC) to degalactosylate GG to form PPG (17). This SGG processing would allow Sertoli cells to continue their roles in supporting the ongoing development of TGCs (13, 19) and, through a recycling process, make available the essential substrate(s) for SGG synthesis by the new generation of testicular germ cells. In this study, we describe the significance of Sertoli cell lysosomal ARSA in these processes using *Arsa*<sup>-/-</sup> mice.

## MATERIALS AND METHODS

### Mice

Details of *Arsa*<sup>-/-</sup> mice with congenic C57BL/6J background were as described (20). Both wild-type and *Arsa*<sup>-/-</sup> mice were bred and housed in our animal facilities, following the protocols approved by the Ottawa Hospital Research Institute Animal Care Committee.

### Mating study

Mating was done with four wild-type and eight *Arsa*<sup>-/-</sup> male mice over a 6-month period starting when the males were ~2 months old. Each male was individually caged with an 8-week-old wild-type female (C57BL/6J) for a duration that the female gave

birth to two litters. Afterwards, the female was replaced with another 8-week-old wild-type female. The replaced females were caged individually for an additional month to ensure that no live births were missed. All the females used were proven fertile by their ability to deliver pups following mating with wild-type males after this 1-month waiting period.

### Sperm-ZP binding and in vitro fertilization

General protocols were as previously described (21). Motile sperm were collected from the swim-up fraction, and an equal number of wild-type and *Arsa*<sup>-/-</sup> sperm were added to medium droplets, each containing 20-30 ovulated eggs retrieved from superovulated wild-type females.

### Histology and transmission electron microscopy

Testis and epididymis sections from wild-type and *Arsa*<sup>-/-</sup> mice were prepared for light and electron microscopy analysis, and profile areas of their seminiferous tubules were quantified and statistically analyzed as previously described (22).

### Detection of apoptotic cells

The terminal deoxynucleotidyl transferase-mediated dUTP nick end labeling (TUNEL) assay was performed on testis sections of wild-type and *Arsa*<sup>-/-</sup> mice. Paraffin sections were deparaffinized and rehydrated serially in decreasing concentrations of ethanol and were permeabilized in 0.1% Triton X-100 in 0.1% sodium citrate [8 min, room temperature (RT)]. After two rinses with PBS, the sections were treated with 1% hydrogen peroxide in 70% ethanol for 10 min to quench endogenous peroxidase activity. Following two washes in PBS, TUNEL staining was carried out using the TUNEL Enzyme and TUNEL Label Mix (Roche Applied Science, Indianapolis, IN) according to the supplier's instructions, and the sections were viewed under an epifluorescence microscope. The fluorescent signals were subsequently converted into colorimetric signals by incubating the sections with anti-fluorescein Fab-peroxidase (POD) complex (Roche) (30 min, 37°C), using a 3,3'-diaminobenzidine (DAB) substrate kit (Vectorlabs, Burlington, ON, Canada), which gave brown staining to positive cells.

### Quantification of SGG from whole testis and sperm lipid extracts

Lipids were extracted from decapsulated testes and PBS-washed epididymal and vas deferens sperm, and then subjected to liquid chromatography ESI-MS/MS and MRM for SGG quantification using deuterated SGG as an internal standard, as previously described (23).

### ESI-MS/MS of glycolipid bands uniquely present in *Arsa*<sup>-/-</sup> testes

Testis lipid extracts from wild-type and *Arsa*<sup>-/-</sup> mice at both 5 and 8 months of age were subjected to high-performance thin layer chromatography (HPTLC) followed by orcinol staining, as previously described (24). Glycolipids were stained purple, whereas phospholipids turned brown. In *Arsa*<sup>-/-</sup> mice, an extra glycolipid band chromatographed between SGG and phosphatidylcholine was observed; the area of the HPTLC plate around this band, starting underneath the SGG band, was scraped for lipid extraction by the Bligh/Dyer method (24). Extracted lipids were subjected to ESI-MS/MS as previously described (23, 25).

### Imaging mass spectrometry

Imaging MS was performed on frozen sections of 8-month-old wild-type and *Arsa*<sup>-/-</sup> testes, which were thaw-mounted onto indium-tin oxide-coated glass slides (Bruker Daltonics, Leipzig,

Germany), using a MALDI-time-of-flight(TOF)/TOF-type instrument, Ultraflex 2 TOF/TOF (Bruker Daltonics), in the negative mode with 2,5-dihydroxybenzoic acid as a matrix, as previously described (26). The spatial resolution of the obtained images was 25  $\mu\text{m}$ .

### Flow cytometry of SGG of TGCs

A testicular germ cell mixture was prepared by sequential enzymatic digestion of seminiferous tubules with collagenase and trypsin. Decapsulated testes were first digested with 0.5 mg/ml collagenase in Dulbecco's Modified Eagle Medium (DMEM, Invitrogen, Burlington, ON, Canada) at 33°C for 15 min with constant shaking at 100 cycles per minute. At the end of the incubation, the dissociated tubules were allowed to sediment by unit gravity and then washed three times with DMEM. The tubules were further digested with 0.5 mg/ml trypsin in DMEM supplemented with 1  $\mu\text{g}/\text{ml}$  of DNase I at 33°C for 15 min with constant shaking at 130 cycles per minute. During the collagenase and trypsin treatments, the tubules were continually flushed with 5%  $\text{CO}_2$ . As a last step, soybean trypsin inhibitor (SBTI) was added to the suspension to a final concentration of 0.5 mg/ml. The suspension was gently processed through a large bore plastic transfer pipet to dissociate small cell clumps and then filtered through a 70  $\mu\text{m}$  nylon screen. The filtered cell suspension was washed three times with washing buffer (0.5% BSA (BSA), 0.25 mg/ml SBTI, 0.5  $\mu\text{g}/\text{ml}$  DNase I in DMEM) by centrifugation (450 g, 5 min). The resulting cell suspension was mainly a mixed population of TGCs, although a certain number of Sertoli cells were unavoidably coisolated.

The isolated testicular germ cells were subjected to flow cytometry. They were first stained with DRAQ5 to differentiate TGC types based on their DNA amounts and/or compactness. Approximately  $2 \times 10^6$  of TGCs in 1 ml of DMEM were incubated (15 min, RT) with 20  $\mu\text{M}$  DRAQ5 (Biostatus, Shephed, Leicestershire, UK). After washing once in PBS by low-speed centrifugation, the cells were fixed with 4% paraformaldehyde in PBS (15 min, RT). Following two washes with PBS supplemented with 0.3% BSA (PBS-BSA), the cells were blocked with 5% normal goat serum and then incubated (45 min, RT) with 5  $\mu\text{g}/\text{ml}$  O4 mouse monoclonal anti-SGG IgM antibody (Neuromics, Edina, MN) or normal mouse IgM diluted in PBS-BSA. The cells were then washed in the same medium and incubated (30 min, RT) with goat anti-mouse IgM conjugated with Alexa 488 fluorochrome (Invitrogen; 1:400 dilution). After washing and resuspending in PBS-BSA, the cells were analyzed on a Coulter EPICS XL flow cytometer (Beckman Coulter Ltd, Mississauga, ON, Canada) equipped with a 15 mW argon laser with excitation at 488 nm. Ten thousand cells from each sample were analyzed at a flow rate of 200-400 cells/second. Fluorescence emission of DRAQ5 (emission  $\lambda_{\text{max}}$  681 nm/697 nm) was quantified in FL4 after passage through a 675 nm bandpass filter (660-700 nm), and SGG fluorescence was reflected by a 550 nm dichroic longpass filter and quantified after transmission through a  $525 \pm 20$  nm bandpass filter.

### Immunofluorescence of intracellular SGG in Sertoli cell cultures

Sertoli cells were isolated from denuded testes of 8-month-old *Arsa*<sup>-/-</sup> and wild-type mice by sequential enzymatic treatments as described (27) and allowed to attach to BD Falcon CultureSlide (BD Biosciences, Mississauga, ON, Canada). Some TGCs were still attached to Sertoli cells even after the culture was treated twice with a hypotonic buffer. Following five days in culture, adherent Sertoli cells were washed in PBS, fixed with 4% paraformaldehyde in PBS (15 min, RT), and treated with 0.1% Triton X-100 in PBS (10 min, RT). After washing twice in PBS and blocking with

5% goat serum in PBS, the fixed and permeabilized Sertoli cells were treated with O4 anti-SGG IgM antibody (5  $\mu\text{g}/\text{ml}$ , 2 h, RT) followed by two washes in PBS and then incubation with Alexa-488 conjugated goat anti-mouse IgM (Invitrogen, 1:400 dilution, 1 h, RT). Fifteen minutes prior to the completion of secondary antibody incubation, 10  $\mu\text{g}/\text{ml}$  of Hoechst 33342 was added to the cell culture to stain the nucleus. The cells were then viewed for SGG staining under an epifluorescence microscope.

### ARSA enzymatic activity assay

Homogenates of Sertoli cells and TGCs in 250 mM acetate buffer, pH 5, were used to assess the desulfation activity of *p*-nitrocathecholsulfate as previously described (28).

### Statistical analyses

Student *t*-test and ANOVA were used to determine significant differences between two data sets.

## RESULTS

### Decreased fecundity and spermatogenesis in older *Arsa*<sup>-/-</sup> males

Natural mating experiments revealed that *Arsa*<sup>-/-</sup> males from 2 to 5 months of age produced the same accumulated numbers of pups per mating pair as age-matched wild-type males. However, at older ages, these parameters were lower for *Arsa*<sup>-/-</sup> males, so that at 8 months of age (equivalent to 40 years in men), it was 65% of the wild-type value (Fig. 1A). Between 2 and 8 months of age, the average litter size that *Arsa*<sup>-/-</sup> males produced from 4.6 litters was  $6.2 \pm 2.4$  pups, as compared with  $7.9 \pm 1.3$  pups from 5.5 litters that were produced by wild-type males ( $P < 0.05$ ). The ability of epididymal and vas deferens sperm from 8-month-old *Arsa*<sup>-/-</sup> males to bind to the ZP and to fertilize eggs in vitro was also minimal compared with sperm from age-matched wild-type males (Fig. 1B). In contrast, sperm-ZP binding and sperm fertilizing ability were the same for *Arsa*<sup>-/-</sup> and wild-type males at 5 months of age (Fig. 1B). Of note was the high number of sperm with abnormal morphology retrieved from 8-month-old *Arsa*<sup>-/-</sup> mice. Even in the swim-up suspension, ~30-40% of these motile sperm had abnormal morphology (Fig. 1C), and this may contribute partly to the decreased fertilizing ability. However, the decreased fecundity was not from the inability of *Arsa*<sup>-/-</sup> males to copulate, as the rate of vaginal plug formation was not noticeably different in females caged with wild-type males versus *Arsa*<sup>-/-</sup> males. Although mild ataxia and ocular problems were observed in some *Arsa*<sup>-/-</sup> male mice at 8 months of age, their body weights (supplemental Table I) and general appearance were similar to those of age-matched wild-type males, and there were no visible indications that their sexual activities were impaired in any way.

Testis histology revealed that spermatogenesis in 8-month-old *Arsa*<sup>-/-</sup> males was compromised with high rates of apoptotic germ cells (Fig. 2B), disorganization of germ cell layers (Fig. 2A) and smaller profile areas of seminiferous tubules (Fig. 2C) compared with age-matched wild-type tubules (Fig. 2A-C). As a result, testis weights and the numbers of sperm produced by 8-month-old

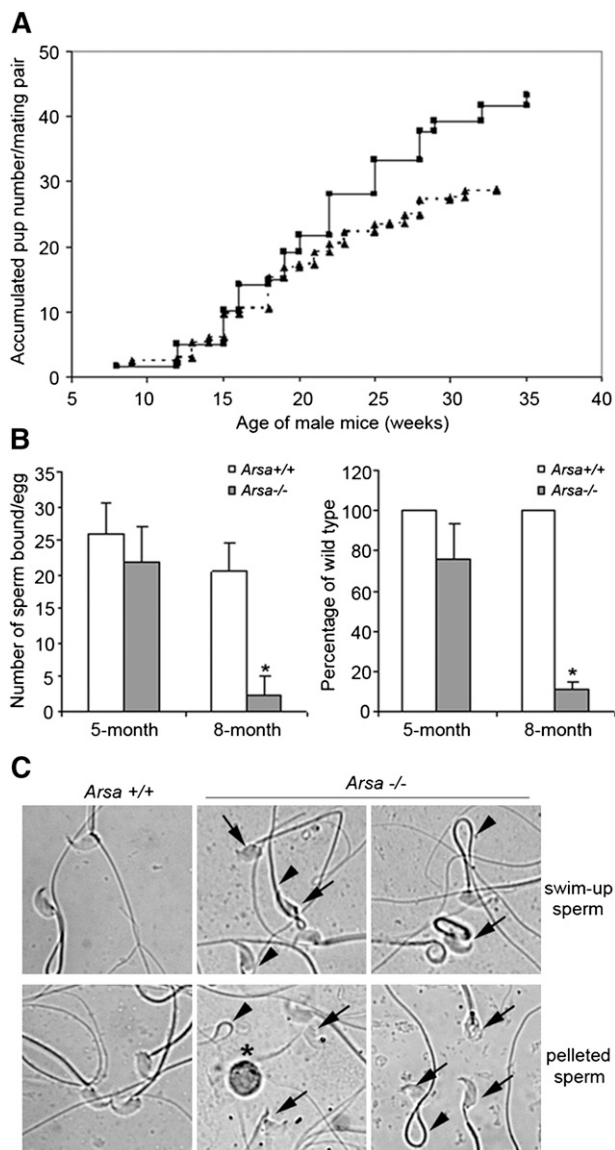


**Fig. 1.** Reduced fecundity of older *Arsa*<sup>-/-</sup> males. **A:** Mating study. At ~2 months of age, four wild-type males and eight *Arsa*<sup>-/-</sup> males were individually caged with 8- to 10-week-old wild-type females for ~6 months. The figure shows lower accumulated numbers of pups sired by *Arsa*<sup>-/-</sup> males (dotted line) compared with wild-type males (solid line). **B:** In vitro sperm-ZP binding and fertilization. Five wild-type and five *Arsa*<sup>-/-</sup> males, each at 5 and 8 months of age, were used in these studies. Data are expressed as mean  $\pm$  SD. Left panel: Number of sperm bound per ZP after 30 min of gamete coincubation. Right panel: Number of eggs fertilized in vitro by motile sperm from *Arsa*<sup>-/-</sup> males expressed as percentages of the values from the age-matched wild-type males, whose sperm consistently fertilized >80% of eggs inseminated. \*Significant difference between *Arsa*<sup>-/-</sup> and *Arsa*<sup>+/+</sup> sperm samples from 8-month-old animals ( $P < 0.005$ ). **C:** Morphology of sperm from 8-month-old wild-type and *Arsa*<sup>-/-</sup> males. Abnormal sperm heads (arrows) were often seen in *Arsa*<sup>-/-</sup> sperm in both the swim-up and pellet fractions. Some *Arsa*<sup>-/-</sup> sperm also showed 180° folding of the tails (arrowheads). Round germ cells (\*) were also present in the pellet fraction.

*Arsa*<sup>-/-</sup> males were only 60% and 50%, respectively, of wild-type males of the same age (Fig. 2D, E). Immature round germ cells were also present in the lumen of the

epididymis of 8-month-old *Arsa*<sup>-/-</sup> mice (Fig. 2A, bottom row, far right panel). However, the epididymal epithelium appeared to be normal (Fig. 2A), and the epididymis and seminal vesicle weights were unchanged from those of wild-type mice (supplemental Table II), results suggesting that the observed abnormalities in spermatogenesis were likely not due to alterations of testosterone levels. In 5-month-old *Arsa*<sup>-/-</sup> males, spermatogenesis and other related parameters were normal (Fig. 2A–E).

### Changes in SGG levels in *Arsa*<sup>-/-</sup> males: SGG accumulation in Sertoli cells lead to a lysosomal storage disorder

As ARSA has been shown to desulfate SGG in vitro (28), SGG levels should be increased in *Arsa*<sup>-/-</sup> mice. As expected, SGG levels, quantified by ESI-MS/MS with multiple reaction monitoring (MRM), were higher in the testes of *Arsa*<sup>-/-</sup> mice at both 5 and 8 months of age compared with age-matched wild-type mice (Fig. 3A). However, levels of epididymal and vas deferens sperm SGG were unchanged in 5 month-old *Arsa*<sup>-/-</sup> males, and they even decreased to 50% of wild-type levels in 8-month-old *Arsa*<sup>-/-</sup> animals (Fig. 3B). SGG levels in *Arsa*<sup>-/-</sup> TGCs at both 5 and 8 months of age were also compared with those of wild-type TGCs by flow cytometry. Primary spermatocytes, round spermatids, and highly condensed elongated spermatids have differential amounts or compactness of DNA. Therefore, by prestaining the TGCs with DRAQ5, a quantitative DNA dye, these cell fractions could be differentiated from each other for analysis of SGG staining intensity (supplemental Fig. I). In 5-month-old mice, SGG levels in primary spermatocytes (SC), round spermatids (RS), and highly condensed elongated spermatids (HC) were similar in *Arsa*<sup>-/-</sup> and wild-type males. However, SGG levels in all three TGC types were decreased compared with the wild-type cells in 8-month-old males, and the decreases in primary spermatocytes and condensing elongated spermatids were statistically significant ( $P < 0.05$ ) (Fig. 3C). Round spermatids, consisting of a number of development steps (steps 1–8 in mice), may contain various amounts of SGG. Although the decreases in SGG levels may have indeed occurred in various round spermatid steps in *Arsa*<sup>-/-</sup> males, the inability to separate the different spermatid steps from each other did not allow for an indication of a significant difference of SGG levels from the wild-type values. Interestingly, C18:0/C16:0 SGG ( $m/z$  823) and C18:1/C16:0 SGG ( $m/z$  821), as well as C16:0 SGC (palmitoylsulfatide,  $m/z$  778), were uniquely present in *Arsa*<sup>-/-</sup> testes in addition to three other SGG species that were normally present in wild-type testes [i.e., the main species, C16:0/C16:0 ( $m/z$  795), and two minor SGG species, C16:0/C14:0 ( $m/z$  767) and C17:0/C16:0 ( $m/z$  809)] (Figs. 4 and 5). All these SGG species and C16:0 SGC utilize the same biosynthesis pathway, indicating that CGT and CST were still active in *Arsa*<sup>-/-</sup> males. In fact, *Cgt* and *Cst* were expressed at similar levels in TGCs of 8-month-old *Arsa*<sup>-/-</sup> and age-matched wild-type mice (supplemental Fig. II).

The increased levels of SGG in 8-month-old *Arsa*<sup>-/-</sup> seminiferous tubules were confirmed by imaging mass

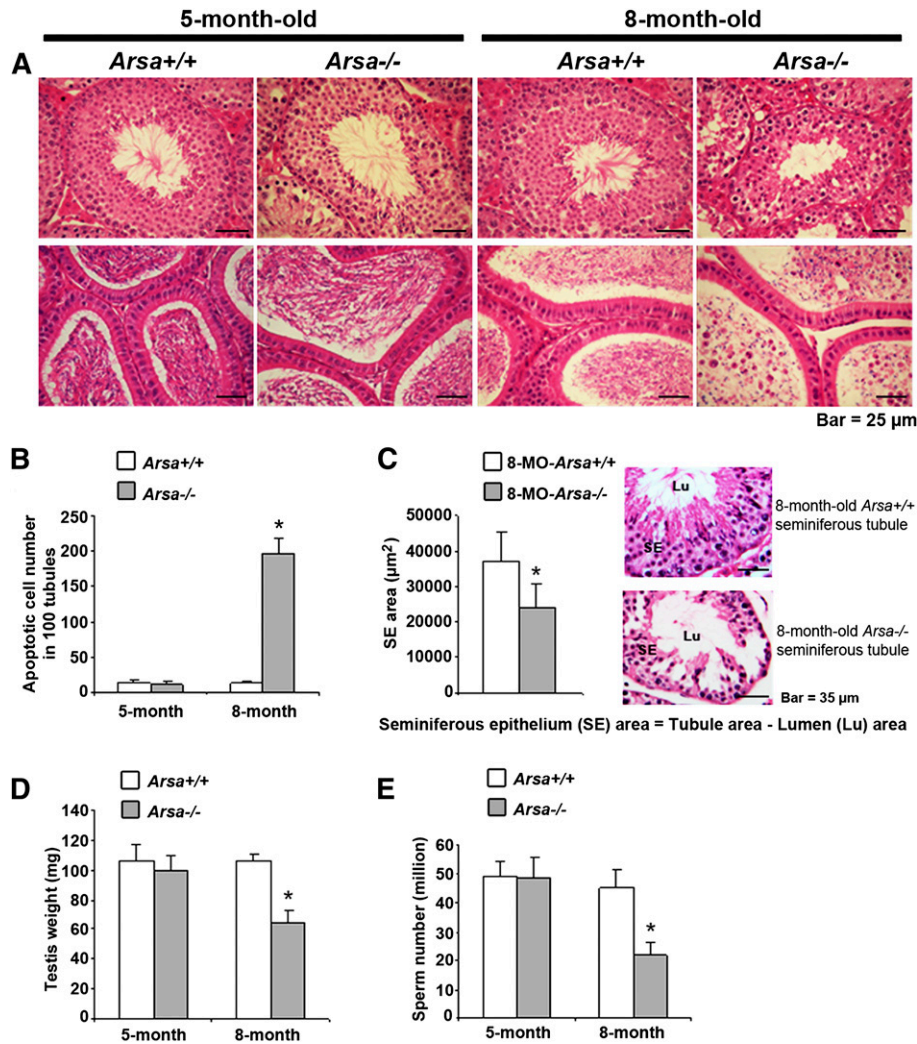


**Fig. 2.** Reduced spermatogenesis in 8-month-old *Arsa*<sup>-/-</sup> males. **A:** Histology of testes (top row) and epididymis (bottom row) of wild-type and *Arsa*<sup>-/-</sup> males at 5 and 8 months of age. Note the disorganization of TGCs in the tubules of 8-month-old mice (top row, far right panel) and the presence of round germ cells in the epididymal lumen, although the epididymal epithelium appeared normal (bottom row, far right panel). In contrast, 5-month-old *Arsa*<sup>-/-</sup> mice showed normal testis and epididymis histology. **B:** Drastic increase in the number of apoptotic germ cells in the tubules of 8-month-old *Arsa*<sup>-/-</sup> males. Quantification was performed in 5 different sets of 100 tubules and expressed as mean  $\pm$  SD per 100 tubules. **C:** Smaller profile areas of the tubules of 8-month-old *Arsa*<sup>-/-</sup> mice compared with age-matched wild-type mice. Quantification was performed on 80 wild-type and 80 *Arsa*<sup>-/-</sup> tubules. **D, E:** Reduced testicular weights and numbers of epididymal and vas deferens sperm in 8-month-old *Arsa*<sup>-/-</sup> mice relative to wild-type mice of the same age. However, these parameters were the same in wild-type and *Arsa*<sup>-/-</sup> mice at 5 months of age. Data in A, B, and C are representative of three replicate experiments, whereas data in D and E are mean  $\pm$  SD of values from five wild-type and five *Arsa*<sup>-/-</sup> mice. \*Significant difference between *Arsa*<sup>-/-</sup> and *Arsa*<sup>+/+</sup> samples from 8-month-old animals;  $P < 0.005$  for B, and  $P < 0.05$  for C, D, and E.

spectrometry (Fig. 4). In the testis, ARSA is present in two cell types, TGCs and Sertoli cells (3). In TGCs, ARSA is synthesized in primary spermatocytes (3, 29) and finally trafficked to the acrosome of spermatids (3). ARSA in Sertoli cells is localized to lysosomes and late residual bodies (3). Notably, the activity of Sertoli cell ARSA was much higher than that of TGCs, as assayed using an artificial substrate, *p*-nitrocatecholsulfate ( $62.65 \pm 8.30$  mU/ $10^6$  cells for Sertoli cells versus  $2.67 \pm 1.12$  mU/ $10^6$  cells for TGCs). Sertoli cell ARSA is likely important for desulfation of SGG in membrane remnants of apoptotic cells and residual bodies that Sertoli cells phagocytose. By deduction, accumulation

of SGG would be in Sertoli cells (Fig. 3D). Immunolocalization of SGG in Triton X-100-treated Sertoli cells isolated from 8-month-old *Arsa*<sup>-/-</sup> and wild-type mice verified this (Fig. 6). SGG staining was at a higher intensity and in larger clumps in *Arsa*<sup>-/-</sup> Sertoli cells than it was in wild-type cells (Fig. 6). These *Arsa*<sup>-/-</sup> Sertoli cells also showed abnormal morphology, including dislocalization of the nucleus and smaller sizes with fewer cellular processes.

Electron microscopy of testis sections revealed further details in the abnormality of Sertoli cells of 8-month-old *Arsa*<sup>-/-</sup> mice. In Sertoli cells of 8-month-old wild-type animals, lysosomes were small dense structures, which varied

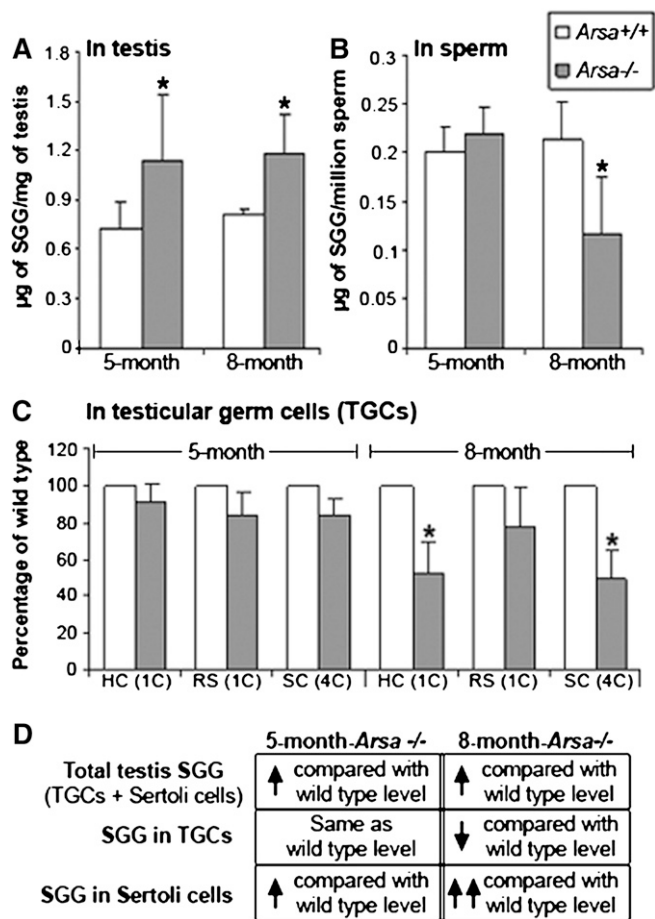


**Fig. 3.** SGG levels in whole testes, sperm, and TGCs from wild-type and *Arsa*<sup>-/-</sup> males at 5 and 8 months of age. SGG was quantified in the lipids extracted from the whole testis (A) and sperm (B) of wild-type and *Arsa*<sup>-/-</sup> mice by ESI-MS/MS-MRM (23). Data are expressed as absolute amounts per milligram testis weight or 1 million sperm. C: SGG levels in various TGC types of *Arsa*<sup>-/-</sup> mice, expressed as percentages of corresponding wild-type TGC values determined by flow cytometry. Three wild-type and three *Arsa*<sup>-/-</sup> mice of both ages were used in A, B, and C, and all data are expressed as mean ± SD. \*Significant difference between *Arsa*<sup>-/-</sup> and *Arsa*<sup>+/+</sup> samples from 8-month-old animals; *P* < 0.05. D: Deduction of results suggesting SGG accumulation in Sertoli cells of *Arsa*<sup>-/-</sup> mice. SC, primary spermatocytes; RS, round spermatids; HC, highly condensed (elongated) spermatids.

in number according to the stages of the spermatogenic cycle (Fig. 7A, panel a), whereas in *Arsa*<sup>-/-</sup> mice, some Sertoli cells had numerous lysosomes with irregular shapes and a heterogeneous content at all stages of the cycle (Fig. 7A, panel b). In other seminiferous tubules, lipid droplets were also apparent in *Arsa*<sup>-/-</sup> Sertoli cells and were especially abundant at Stages I-VII of the cycle (Fig. 7A, panel c). Such droplets were not found in wild-type Sertoli cells. In some tubules, lysosomes of Sertoli cells of *Arsa*<sup>-/-</sup> mice were very large, more or less spherical, and numerous, contrasting the smaller uniform sizes of Sertoli lysosomes of wild-type mice (Fig. 7A, panel d). These abnormal appearances in *Arsa*<sup>-/-</sup> Sertoli cells were typical of a lysosomal storage disorder (17, 18), which likely contributed to Sertoli cell dysfunction. In normal testes, Sertoli cells provide spatial support to developing TGCs: they cytoorganize the more advanced TGCs to localize closer to the

tubal lumen, and the heads of elongated spermatids are positioned vertically to the basement membrane (19). In the tubules of 8-month-old *Arsa*<sup>-/-</sup> mice, several elongated spermatid heads were disoriented, lying horizontal to the basement membrane (Fig. 7B, upper panel). The phagocytic function of Sertoli cells for “cleaning up” apoptotic germ cells was also impaired in 8-month-old *Arsa*<sup>-/-</sup> mice. Apoptotic germ cells were frequently present in *Arsa*<sup>-/-</sup> tubules (Fig. 7B, lower panel), whereas they were not abundant in wild-type testes.

## DISCUSSION

The ability of ARSA to desulfate SGC and SGG in the presence of saposin B has been well characterized in vitro (1), and for SGC, it has been confirmed in vivo (2, 30). In this study, we revealed that SGG accumulation occurred in Sertoli cells of *Arsa*<sup>-/-</sup> mice, indicating that SGG was also a physiological substrate of enzymatically active ARSA in Sertoli cell lysosomes. Presumably, saposin B, which is essential for delivering “solubilized” SGG into the active site pocket of ARSA, is also produced by Sertoli cells, as prosaposin is de novo synthesized in these cells (31) and can be cleaved to saposin B by cathepsin D (32), which is also present in Sertoli cell lysosomes (33). As the major glycolipid of male germ cells, the degradation pathway for SGG in Sertoli cells may be essential for the process of spermatogenesis, as apoptosis occurs at >50% of total germ cell population in normal mice (13). These apoptotic germ cells are usually phagocytosed by Sertoli cells (34), and their subcellular components, especially those that are cytotoxic, need to be processed after phagocytosis. Once phagocytosed within the Sertoli cell, apoptotic germ cell fragments presumably fuse with the Sertoli cell lysosomes for the degradation reactions (14). Such events in normal mice and rats must be rapid and efficient, as examples of this phenomenon are rarely seen (34, 35). A similar process also occurs with residual bodies (36). However, the latter are numerous, rendering evidence of phagocytosis and the involvement of Sertoli lysosomes in this degradation process (36).

Phagocytic activity of Sertoli cells is likely enhanced by preferential internalization of acidic lipids (e.g., phosphatidylserine (37)) present on the surface of apoptotic germ cells. Negatively charged SGG is also preferentially internalized into Sertoli cells, even at a higher capacity than phosphatidylserine (supplemental Fig. III). This “eat me” signal of SGG may reflect the need for SGG degradation in Sertoli cells. Like its analog SGC, SGG may be cytotoxic when present intracellularly at aberrantly high levels (16). Because Sertoli cells and male germ cells contain lipases (38–40), lyso-SGG may be produced following the intracellular accumulation of SGG in *Arsa*<sup>-/-</sup> testes. Lyso-glycolipids are believed to be more cytotoxic than the parental lipids (18). Psychosine (galactosylsphingosine) is one such lyso-glycolipid, which is accumulated in the brain of galactosylceramidase-depleted Krabbe patients and twitcher mice, resulting in severe dys/demyelination (18, 41, 42). HPTLC of lipid extracts from both testis and

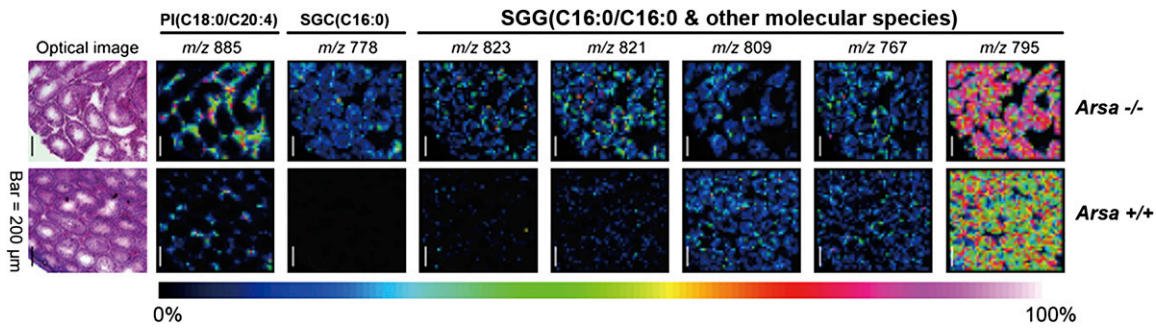


**Fig. 4.** Imaging mass spectrometry analyses of frozen testis sections from 8-month-old wild-type and *Arsa*<sup>-/-</sup> mice. The number of laser irradiations was 200 shots in each spot, and the raster width was 25 μm. FlexImaging 2.0 software was used to reconstruct ion images. Both *Arsa*<sup>-/-</sup> and *Arsa*<sup>+/+</sup> samples were analyzed at the same time. The total ion current of each raster point was normalized for semiquantitative analyses. The signal at *m/z* 795 was attributed to the main SGG species (C16:0/C16:0). Other SGG molecular species include C16:0/C14:0 at *m/z* 767, C17:0/C16:0 at *m/z* 809, C18:1/C16:0 at *m/z* 821, and C18:0/C16:0 at *m/z* 823. The ion at *m/z* 885 was attributed to phosphatidylinositol (PI; C18:0/C20:4); it is selectively present in the interstitial space and was used to aid the localization of the tubule periphery. Results shown are representative of three wild-type and three *Arsa*<sup>-/-</sup> mice. The ion at *m/z* 778 was attributed to SGC (C16:0), the structure of which was confirmed by ESI-MS/MS analysis (see Fig. 5). The presence of C16:0 SGC, C18:1/C16:0 SGG, and C18:0/C16:0 SGG in the tubules was specific to *Arsa*<sup>-/-</sup> mice.

sperm homogenates failed to reveal the lyso-SGG band. Furthermore, ESI-MS analyses revealed that lyso-SGG (*m/z* 556.6) was present in the testis homogenate of *Arsa*<sup>-/-</sup> mice at very low levels (from undetected to 4% of SGG), and consistently, the wild-type testis homogenates contained undetectable amounts of lyso-SGG (supplemental

Fig. IV). In sperm, lyso-SGG was undetected in both wild-type and *Arsa*<sup>-/-</sup> mice. All these results argued strongly that the impairment of spermatogenesis and sperm fertilizing ability was a consequence of the changes of SGG levels, and not its lyso form, in Sertoli cells and male germ cells.

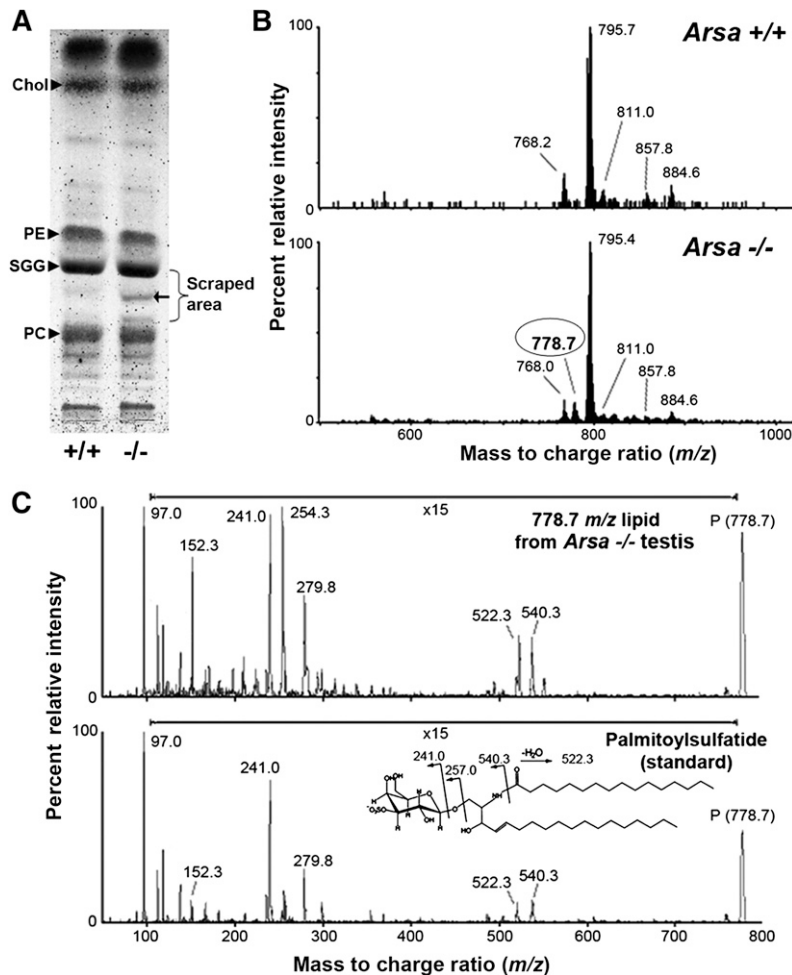


**Fig. 5.** C16:0 SGC (palmitoylsulfatide) was present in the testis of *Arsa*<sup>-/-</sup> mice at 8 months of age. **A:** HPTLC of testis lipids from wild-type and *Arsa*<sup>-/-</sup> mice. Lipid standards, including cholesterol (Chol), phosphatidylcholine (PC), SGG, and phosphatidylethanolamine (PE), were also loaded. An extra glycolipid band (arrow) was detected in the *Arsa*<sup>-/-</sup> testis sample. The area surrounding this glycolipid band (denoted by a bracket) was scraped separately from *Arsa*<sup>-/-</sup> and wild-type lanes. Lipids in the silica powder were extracted by the Bligh/Dyer method (24) and subjected to ESI-MS in the negative ion mode. **B:** ESI-MS spectra revealed that the *m/z* 778.7 ion peak existed only in the *Arsa*<sup>-/-</sup> sample; this signal is consistent with palmitoylsulfatide. **C:** ESI-MS/MS of the *m/z* 778.7 lipid purified from *Arsa*<sup>-/-</sup> testis and palmitoylsulfatide standard (Matreya, Pleasant Gap, PA) show high similarity of fragmentation patterns, indicating that the *m/z* 778.7 ion in *Arsa*<sup>-/-</sup> testis was palmitoylsulfatide. The data shown are representative of three *Arsa*<sup>-/-</sup> mice.

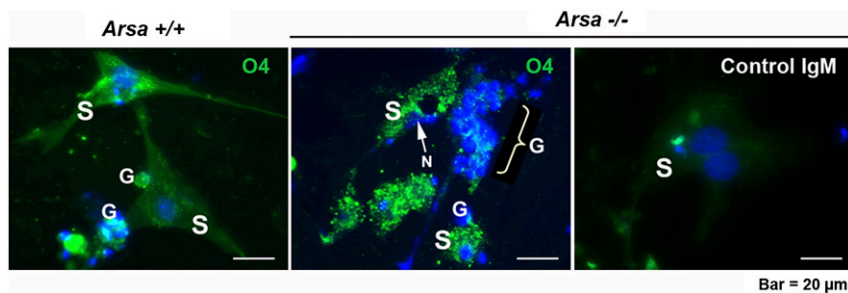


**Fig. 6.** Higher levels of intracellular SGG in Sertoli cells from *Arsa*<sup>-/-</sup> males, relative to wild-type males, at 8 months of age. Sertoli cells (S) were isolated from 8-month-old wild-type and *Arsa*<sup>-/-</sup> mice. Some germ cells (G) were coisolated. Cells were aldehyde-fixed and treated with 0.1% Triton X-100 followed by indirect immunofluorescence for SGG detection. Note the intracellular staining of SGG in Sertoli cells of both wild-type and *Arsa*<sup>-/-</sup> mice; however, the staining was more intense and appeared as clumped patterns in the knockout mice. SGG on the surface of germ cells was absent due to the Triton X-100 extraction. The nucleus (N) of *Arsa*<sup>-/-</sup> Sertoli cells was often positioned at a wrong site (representatively pointed to by a white arrow in the center panel). The right panel shows a negative control of background fluorescence staining with normal mouse IgM. Nuclei were localized by Hoechst 33342. Results shown are representative of three wild-type and three *Arsa*<sup>-/-</sup> mice.

In *Arsa*<sup>-/-</sup> mice, SGG accumulation over time in Sertoli cells may be a direct and/or indirect cause for lysosomal swelling observed in these cells, a common feature of a lysosomal storage disorder. This disorder may lead to functional defects, including the spatial and nutritional support that Sertoli cells provide to developing germ cells during spermatogenesis (13, 19). In 8-month-old *Arsa*<sup>-/-</sup> mice, the orientation of spermatid heads was often abnormal; they were positioned horizontally instead of vertically to the basement membrane. Abnormal morphology of the sperm heads was also observed at high rates in these older *Arsa*<sup>-/-</sup> mice. These abnormalities may be associated with defective formation of the apical ectoplasmic specialization in Sertoli cells, a device for anchoring and shaping of the elongated spermatid heads (13). Furthermore, the phagocytic function of Sertoli cells may be compromised in 8-month-old *Arsa*<sup>-/-</sup> mice due to increased numbers of apoptotic germ cells, as well as the inability of Sertoli cells to effectively deal with this increased load. It is known that Sertoli cells can only support a finite number of germ cells (13, 43), and an increased workload could disturb this

delicate balance. With a drastic increase in apoptotic cell numbers in 8-month-old *Arsa*<sup>-/-</sup> mice, their Sertoli cells were likely unable to maintain their normal functions in preserving the integrity of the seminiferous tubules. Nonetheless, all these abnormalities associated with spermatogenesis were unlikely to result from altered levels of circulating and luminal androgens, as the morphology of the epididymal epithelium, a target tissue of androgens, as well as epididymal and seminal vesicle weights, were normal in 8-month-old *Arsa*<sup>-/-</sup> mice (supplemental Table II).

The lower levels of SGG in TGCs and in sperm of 8-month-old *Arsa*<sup>-/-</sup> mice may be a factor related to reduced spermatogenesis and marked decrease in sperm fertilizing ability, respectively. SGG on the testicular germ cell surface is essential for spermatogenesis (11, 12). For sperm surface SGG, our accumulated findings indicate that it has direct affinity for the ZP and is involved in the binding between acrosome intact sperm and the ZP (7, 8). In addition, SGG on the acrosome-reacted sperm head plays roles in sperm-egg plasma membrane interaction (44). SGG is also an integral component of sperm head

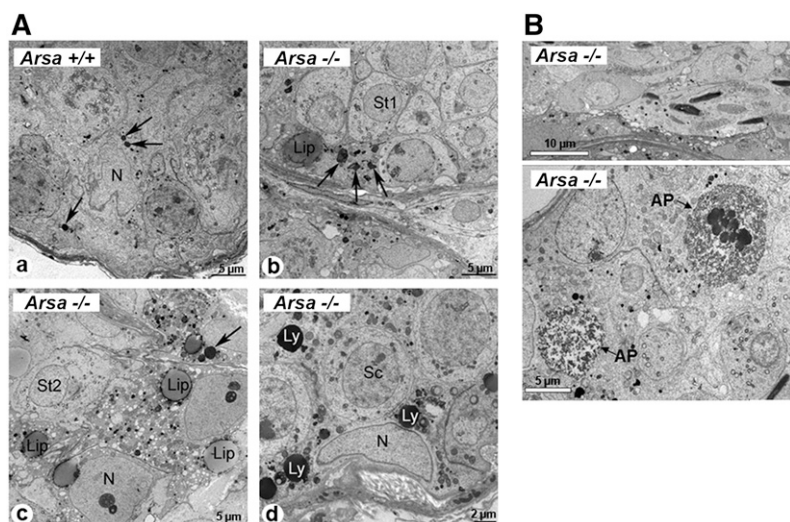


**Fig. 7.** Electron microscopy of testis sections of 8-month-old wild-type and *Arsa*<sup>-/-</sup> males. A: In normal Sertoli cells, lysosomes (arrows) appeared as small dense structures (a). In *Arsa*<sup>-/-</sup> mice, Sertoli cells had numerous lysosomes (arrows) with irregular shapes and heterogeneous content (b) or enlarged spherical structures (Ly, d). Lipid droplets (Lip) were also apparent in some *Arsa*<sup>-/-</sup> Sertoli cells (c). N, nucleus; Sc, spermatocyte; St, spermatid. B: Disorientation of elongated sperm heads in the seminiferous tubules of 8-month-old *Arsa*<sup>-/-</sup>; they were horizontal to the basement membrane instead of being vertical as expected in the normal testis (upper panel). Presence of a high number of apoptotic germ cells (AP) in the tubules of 8-month-old *Arsa*<sup>-/-</sup> mice (lower panel). Results are representative of five wild-type and five *Arsa*<sup>-/-</sup> mice.



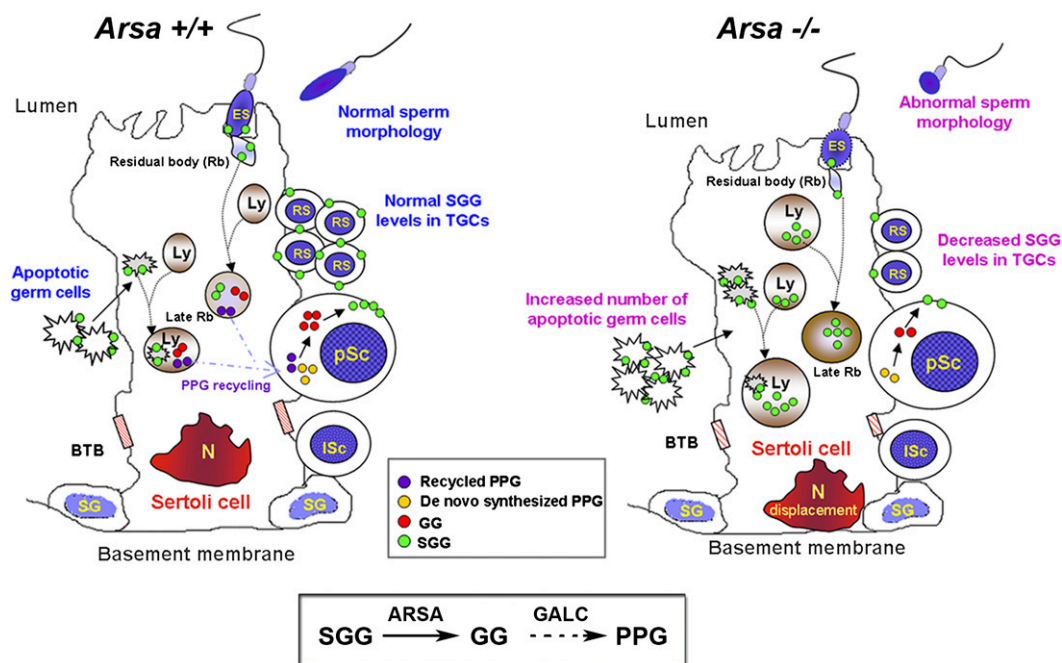


**Fig. 8.** SGG homeostasis in seminiferous tubules of wild-type and 8-month-old *Arsa*<sup>-/-</sup> mice. Left: Sertoli cells of normal testes degrade SGG from apoptotic germ cells and residual bodies to galactosylglycerolipid (GG) by ARSA and then to PPG by GALC (see box). The generated PPG may be recycled to developing pachytene spermatocytes (pSc) for new SGG biosynthesis, although pSc would also synthesize PPG de novo. Right: In 8-month-old *Arsa*<sup>-/-</sup> mice, Sertoli cells fail to degrade SGG, leading to its accumulation in the lysosomes, which then become swollen, a phenomenon typical of a lysosomal storage disorder. The SGG accumulation may result in cytotoxicity and subsequent decreases in functionality of Sertoli cells. This likely includes reduced ability to phagocytose apoptotic germ cells and to support development of germ cells in the adluminal compartment. pSc may then synthesize less PPG. Together with the lack of the recycling PPG pool from Sertoli cells, germ cells contain decreased SGG levels. The cytotoxicity of accumulated SGG in Sertoli cells of 8-month-old *Arsa*<sup>-/-</sup> includes displacement of the Sertoli cell nucleus (N). BTB, blood-testis barrier; ES, elongated spermatid; ISc, leptotene spermatocyte; Ly, lysosome; RS, round spermatid; SG, spermatogonium. Box: Degradation pathway of SGG in Sertoli cells. The first step of SGG desulfation by ARSA was demonstrated in this study. The degalactosylation step of GG by GALC remains to be verified.

lipid rafts, which contain a number of ZP binding proteins, including ARSA, and are thus platforms for ZP binding (5, 6). Our results revealed normal *in vitro* fertilizing ability and SGG levels in sperm from 5-month-old *Arsa*<sup>-/-</sup> mice, but near-zero fertilizing ability and a 50% decrease in sperm SGG levels in 8-month-old *Arsa*<sup>-/-</sup> animals. This indicated that sperm ARSA was dispensable for sperm fertilizing ability, whereas normal levels of sperm SGG was essential for *in vitro* fertilization. However, 8-month-old *Arsa*<sup>-/-</sup> males still sired offspring, although at a reduced rate compared with age-matched wild-type males. This result argued that the *Arsa*<sup>-/-</sup> sperm may be partly rescued in the female reproductive tract, as in the case of sperm genetically null for a surface serine protease, Prss21 (45). Nonetheless, the reduced rate of spermatogenesis and fecundity together with altered levels of SGG in the testis and sperm in 8-month-old *Arsa*<sup>-/-</sup> mice strongly suggests that homeostasis of SGG is important for male fertility, especially at advancing ages.

The decreases in SGG levels in TGCs and sperm in 8-month-old *Arsa*<sup>-/-</sup> mice were unexpected, considering that ARSA is a SGG degradation enzyme. The reduced

SGG levels in germ cells could arise from decreased activities of CGT and CST in the knockout mice to synthesize SGG, although both enzymes were still expressed at a similar transcriptional level in 8-month-old *Arsa*<sup>-/-</sup> and wild-type testes (supplemental Fig. II). Alternatively, the reduced SGG levels in TGCs of 8-month-old *Arsa*<sup>-/-</sup> mice may be due to limited supplies of the initial substrate, palmitoylpalmitoylglycerol (PPG), required for SGG biosynthesis. In normal testes, PPG may be de novo synthesized within TGCs as well as transported from Sertoli cells following SGG degradation by ARSA to GG, which in turn is processed to PPG by GALC, which is also present in Sertoli cells (supplemental Fig. V). In *Arsa*<sup>-/-</sup> mice, this PPG recycling pool will not be available, although at a younger age, TGCs may compensate for this missing pool of PPG by increasing de novo synthesis. This compensation may not be possible in 8-month-old *Arsa*<sup>-/-</sup> mice, leading to decreased SGG levels in germ cells.

Our results on *Arsa*<sup>-/-</sup> mice have revealed the significance of SGG homeostasis for male fertility, and a model explaining the link between the SGG biosynthesis and degradation processes is shown (Fig. 8). While the biosynthesis

pathway has been well documented (8), this study describes for the first time the initial part of the SGG degradation pathway regulated by Sertoli cell lysosomal ARSA. The degradation of SGG from apoptotic germ cells may serve dual purposes: to prevent SGG-induced cytotoxicity and to generate a neutral lipid intermediate, PPG, for SGG synthesis in new generations of primary spermatocytes. **■**

The authors acknowledge the assistance of T. van Gulik in manuscript preparation.

## REFERENCES

- Hanson, S. R., M. D. Best, and C. H. Wong. 2004. Sulfatases: structure, mechanism, biological activity, inhibition, and synthetic utility. *Angew. Chem. Int. Ed. Engl.* **43**: 5736–5763.
- Gieselmann, V. 2008. Metachromatic leukodystrophy: genetics, pathogenesis and therapeutic options. *Acta Paediatr. Suppl.* **97**: 15–21.
- Weerachatanukul, W., H. Xu, A. Anupriwan, E. Carmona, M. Wade, L. Hermo, S. M. da Silva, P. Rippstein, P. Sobhon, P. Sretarugsa, et al. 2003. Acquisition of arylsulfatase A onto the mouse sperm surface during epididymal transit. *Biol. Reprod.* **69**: 1183–1192.
- Carmona, E., W. Weerachatanukul, H. Xu, A. L. Fluharty, A. Anupriwan, A. Shoushtarian, K. Chakrabandhu, and N. Tanphaichitr. 2002. Binding of arylsulfatase A to mouse sperm inhibits gamete interaction and induces the acrosome reaction. *Biol. Reprod.* **66**: 1820–1827.
- Bou Khalil, M., K. Chakrabandhu, H. Xu, W. Weerachatanukul, M. Buhr, T. Berger, E. Carmona, N. Vuong, P. Kumarathasan, P. T. Wong, et al. 2006. Sperm capacitation induces an increase in lipid rafts having zona pellucida binding ability and containing sulfogalactosylglycerolipid. *Dev. Biol.* **290**: 220–235.
- Nixon, B., A. Bielanowicz, E. A. McLaughlin, N. Tanphaichitr, M. A. Ensslin, and R. J. Aitken. 2009. Composition and significance of detergent resistant membranes in mouse spermatozoa. *J. Cell. Physiol.* **218**: 122–134.
- Tanphaichitr, N., E. Carmona, M. Bou Khalil, H. Xu, T. Berger, and G. L. Gerton. 2007. New insights into sperm-zona pellucida interaction: involvement of sperm lipid rafts. *Front. Biosci.* **12**: 1748–1766.
- Tanphaichitr, N., M. Bou Khalil, W. Weerachatanukul, M. Kates, H. Xu, E. Carmona, M. Attar, and D. Carrier. 2003. Physiological and biophysical properties of male germ cell sulfogalactosylglycerolipid. In *Lipid Metabolism and Male Fertility*. S. De Vriese, editor. AOCS Press, Champaign, IL. 125–148.
- Kornblatt, M. J. 1979. Synthesis and turnover of sulfogalactosylglycerolipid, a membrane lipid, during spermatogenesis. *Can. J. Biochem.* **57**: 255–258.
- Knapp, A., M. J. Kornblatt, H. Schachter, and R. K. Murray. 1973. Studies on the biosynthesis of testicular sulfoglycerogalactolipid: demonstration of a Golgi-associated sulfotransferase activity. *Biochem. Biophys. Res. Commun.* **55**: 179–186.
- Fujimoto, H., K. Tadano-Aritomi, A. Tokumasu, K. Ito, T. Hikita, K. Suzuki, and I. Ishizuka. 2000. Requirement of seminolipid in spermatogenesis revealed by UDP-galactose:ceramide galactosyltransferase-deficient mice. *J. Biol. Chem.* **275**: 22623–22626.
- Honke, K., Y. Hirahara, J. Dupree, K. Suzuki, B. Popko, K. Fukushima, J. Fukushima, T. Nagasawa, N. Yoshida, Y. Wada, et al. 2002. Paranodal junction formation and spermatogenesis require sulfoglycolipids. *Proc. Natl. Acad. Sci. USA.* **99**: 4227–4232.
- Cheng, C. Y., and D. D. Mruk. 2010. A local autocrine axis in the testes that regulates spermatogenesis. *Nat. Rev. Endocrinol.* **6**: 380–395.
- Clermont, Y., C. Morales, and L. Hermo. 1987. Endocytic activities of Sertoli cells in the rat. *Ann. N. Y. Acad. Sci.* **513**: 1–15.
- Nakanishi, Y., and A. Shiratsuchi. 2004. Phagocytic removal of apoptotic spermatogenic cells by Sertoli cells: mechanisms and consequences. *Biol. Pharm. Bull.* **27**: 13–16.
- Zeng, Y., H. Cheng, X. Jiang, and X. Han. 2008. Endosomes and lysosomes play distinct roles in sulfatide-induced neuroblastoma apoptosis: potential mechanisms contributing to abnormal sulfatide metabolism in related neuronal diseases. *Biochem. J.* **410**: 81–92.
- Schulze, H., T. Kolter, and K. Sandhoff. 2009. Principles of lysosomal membrane degradation: Cellular topology and biochemistry of lysosomal lipid degradation. *Biochim. Biophys. Acta.* **1793**: 674–683.
- Xu, Y. H., S. Barnes, Y. Sun, and G. A. Grabowski. 2010. Multi-system disorders of glycosphingolipid and ganglioside metabolism. *J. Lipid Res.* **51**: 1643–1675.
- Griswold, M. D., and D. McLean. 2006. The Sertoli cell. In *Knobil and Neill's Physiology of Reproduction*. J. D. Neill, T. M. Plant, D. W. Pfaff, J. R. G. Challis, D. M. de Kretser, J. S. Richards, and P. M. Wassarman, editors. Elsevier, New York. 949–975.
- Wu, A., A. Anupriwan, S. Iamsaard, K. Chakrabandhu, D. C. Santos, T. Rupar, B. K. Tsang, E. Carmona, and N. Tanphaichitr. 2007. Sperm surface arylsulfatase A can disperse the cumulus matrix of cumulus oocyte complexes. *J. Cell. Physiol.* **213**: 201–211.
- Tantibhedhyangkul, J., W. Weerachatanukul, E. Carmona, H. Xu, A. Anupriwan, D. Michaud, and N. Tanphaichitr. 2002. Role of sperm surface arylsulfatase A in mouse sperm-zona pellucida binding. *Biol. Reprod.* **67**: 212–219.
- Korah, N., C. E. Smith, A. d'Azzo, M. El Alfy, and L. Hermo. 2003. Increase in macrophages in the testis of cathepsin a deficient mice suggests an important role for these cells in the interstitial space of this tissue. *Mol. Reprod. Dev.* **64**: 302–320.
- Kongmanas, K., H. Xu, A. Yaghoobian, L. Franchini, L. Panza, F. Ronchetti, K. F. Faull, and N. Tanphaichitr. 2010. Quantification of seminolipid by LC-ESI-MS/MS-multiple reaction monitoring: compensatory levels in *Cg1<sup>-/-</sup>* mice. *J. Lipid Res.* **51**: 3548–3558.
- Anupriwan, A., M. Schenk, K. Kongmanas, R. Vanichviriyakit, D. Costa Santos, A. Wu, A. Yaghoobian, T. Berger, P.-G. Nyholm, K. F. Faull, et al. 2008. Presence of arylsulfatases in mouse ovaries: Localization of arylsulfatase A to the corpus luteum. *Endocrinology.* **149**: 3942–3951.
- Franchini, L., L. Panza, K. Kongmanas, N. Tanphaichitr, K. F. Faull, and F. Ronchetti. 2008. An efficient and convenient synthesis of deuterium-labelled seminolipid isotopomers and their ESI-MS characterization. *Chem. Phys. Lipids.* **152**: 78–85.
- Goto-Inoue, N., T. Hayasaka, N. Zaima, and M. Setou. 2009. The specific localization of seminolipid molecular species on mouse testis during testicular maturation revealed by imaging mass spectrometry. *Glycobiology.* **19**: 950–957.
- Lee, W. M., C. Y. Cheng, C. W. Bardin, G. L. Gunsalus, and N. A. Musto. 1986. Measurement of a follicle-stimulating hormone-responsive protein of Sertoli cell origin using an enzyme-linked immunoblot assay. *Endocrinology.* **119**: 1914–1921.
- Schenk, M., C. A. Koppisetty, D. C. Santos, E. Carmona, S. Bhatia, P. G. Nyholm, and N. Tanphaichitr. 2009. Interaction of arylsulfatase-A (ASA) with its natural sulfoglycolipid substrates: a computational and site-directed mutagenesis study. *Glycoconj. J.* **26**: 1029–1045.
- Kreysing, J., A. Polten, G. Lukatela, U. Matzner, K. van Figura, and V. Gieselmann. 1994. Translational control of arylsulfatase A expression in mouse testis. *J. Biol. Chem.* **269**: 23255–23261.
- Stroobants, S., T. Leroy, M. Eckhardt, J. M. Aerts, D. Berckmans, and R. D'Hooge. 2008. Early signs of neurolipidosis-related behavioural alterations in a murine model of metachromatic leukodystrophy. *Behav. Brain Res.* **189**: 306–316.
- Igdoura, S. A., A. Rasky, and C. R. Morales. 1996. Trafficking of sulfated glycoprotein-1 (prosaposin) to lysosomes or to the extracellular space in rat Sertoli cells. *Cell Tissue Res.* **283**: 385–394.
- Hiraiwa, M., B. M. Martin, Y. Kishimoto, G. E. Conner, S. Tsuji, and J. S. O'Brien. 1997. Lysosomal proteolysis of prosaposin, the precursor of saposins (sphingolipid activator proteins): its mechanism and inhibition by ganglioside. *Arch. Biochem. Biophys.* **341**: 17–24.
- Chung, S. S. W., L. J. Zhu, M. Y. Mo, B. Silvestrini, W. M. Lee, and C. Y. Cheng. 1998. Evidence for cross-talk between sertoli and germ cells using selected cathepsins as markers. *J. Androl.* **19**: 686–703.
- Russell, D. L., R. Ettl, A. P. Sinka Hikim, and E. D. Clegg. 1990. *Historical and Histopathological Evaluation of the Testis*. Cache River Press, Vienna, IL.
- Kerr, J. B., K. L. Loveland, M. K. O'Bryan, and D. M. de Kretser. 2006. Cytology of the testis and intrinsic control mechanisms. In *Knobil and Neill's Physiology of Reproduction*. J. D. Neill, T. M. Plant, D. W. Pfaff, J. R. G. Challis, and D. M. de Kretser, J. S. Richards, and P. M. Wassarman, editors. Elsevier, New York. 827–947.

36. Morales, C., Y. Clermont, and L. Hermo. 1985. Nature and function of endocytosis in Sertoli cells of the rat. *Am. J. Anat.* **173**: 203–217.
37. Kawasaki, Y., A. Nakagawa, K. Nagaosa, A. Shiratsuchi, and Y. Nakanishi. 2002. Phosphatidylserine binding of class B scavenger receptor type I, a phagocytosis receptor of testicular sertoli cells. *J. Biol. Chem.* **277**: 27559–27566.
38. Kabbaj, O., C. Holm, M. L. Vitale, and R. M. Pelletier. 2001. Expression, activity, and subcellular localization of testicular hormone-sensitive lipase during postnatal development in the guinea pig. *Biol. Reprod.* **65**: 601–612.
39. Nielsen, J. E., M. L. Lindegaard, L. Friis-Hansen, K. Almstrup, H. Leffers, L. B. Nielsen, and E. Rajpert-De Meyts. 2010. Lipoprotein lipase and endothelial lipase in human testis and in germ cell neoplasms. *Int. J. Androl.* **33**: e207–e215.
40. Yuan, Y. Y., W. Y. Chen, Q. X. Shi, L. Z. Mao, S. Q. Yu, X. Fang, and E. R. Roldan. 2003. Zona pellucida induces activation of phospholipase a(2) during acrosomal exocytosis in guinea pig spermatozoa. *Biol. Reprod.* **68**: 904–913.
41. Matsuda, J., and K. Suzuki. Krabbe disease (globoid cell leukodystrophy). 2007. *In Lysosomal Storage Disorders*. J. A. Barranger and M. A. Cabrera-Salazar, editors. Springer, New York. 269–283.
42. Igisu, H., and K. Suzuki. 1984. Progressive accumulation of toxic metabolite in a genetic leukodystrophy. *Science.* **224**: 753–755.
43. Hermo, L., R. M. Pelletier, D. G. Cyr, and C. E. Smith. 2010. Surfing the wave, cycle, life history, and genes/proteins expressed by testicular germ cells. Part I: background to spermatogenesis, spermatogonia, and spermatocytes. *Microsc. Res. Tech.* **73**: 241–278.
44. Ahnonkitpanit, V., D. White, S. Suwajanakorn, F. Kan, M. Namking, G. Wells, and N. Tanphaichitr. 1999. Role of egg sulfolipidimmobilizing protein 1 (SLIP1) on sperm-egg plasma membrane binding. *Biol. Reprod.* **61**: 749–756.
45. Yamashita, M., A. Honda, A. Ogura, S. Kashiwabara, K. Fukami, and T. Baba. 2008. Reduced fertility of mouse epididymal sperm lacking Prss21/Tesp5 is rescued by sperm exposure to uterine microenvironment. *Genes Cells.* **13**: 1001–1013.